STRUCTURAL STUDY OF LANGMUIR-BLODGETT MONOLAYERS AND MULTILAYERS OF AMYLOSE-ESTERS WITH VARIOUS ALKYL CHAINS

SCHOONDORP, MA; VORENKAMP, EJ; SCHOUTEN, AJ

Published in:
Thin Solid Films

DOI:
10.1016/0040-6090(91)90180-6

Publication date:
1991

Thin Solid Films, *196* (1991) 121–136
LANGMUIR-BLODGETT AND RELATED FILMS

STRUCTURAL STUDY OF LANGMUIR–BLODGETT MONOLAYERS AND MULTILAYERS OF AMYLOSE-ESTERS WITH VARIOUS ALKYL CHAINS

M. A. SCHOONDORP, E. J. VORENKAMP AND A. J. SCHOUTEN
State University of Groningen, Department of Polymer Chemistry, Nijenborgh 16, 9747 AG Groningen (The Netherlands)
(Received March 21, 1990; revised June 13, 1990; accepted July 17, 1990)

A series of amylose-esters with various side chain lengths was studied. Isotherms of the monolayers on the water surface were measured, and polarized IR measurements, small-angle X-ray scattering, and ellipsometric measurements were carried out in order to characterize the structure of the multilayers formed. Amylose-esters with short alkyl side chains appear to have a helical conformation on the water surface which can be transferred into multilayers. The amylose-palmitate ester, however, as an example of an amylose-ester with long alkyl side chains, can only be transferred into mulilayers when the degree of substitution is lower than about 2.3 and only then when the monolayer is in the liquid analogous state to some extent. Amylose-palmitate forms partly ordered Y-type multilayers with side-chains that have a preferential orientation perpendicular to the surface.

1. INTRODUCTION

Recently there has been renewed interest in the field of Langmuir–Blodgett (LB) films of preformed polymers, because of their degree of order and mechanical and thermal stability[1–3]. The behaviour of some preformed polymers on the water surface was studied as early as 1924[4], and later on a systematic study of several polymers was carried out by Crisp[5]. Monolayer transfer of preformed polymers to form multilayers on a substrate was only studied in detail recently for some specific systems[6–12].

Initially, preformed polymers with distinct hydrophobic and hydrophilic parts, analogous to low molecular weight amphiphilic molecules, were investigated. Tredgold has given a review on polymeric LB materials other than strictly amphiphilic[13]. It is known that poly(γ-methyl-*L*-glutamate), poly(γ-benzyl-*L*-glutamate) and copolymers of γ-methyl-*L*-glutamate and γ-benzyl-*L*-glutamate form LB multilayers built up with α-helices[14–16]. Strictly speaking, these helices are not amphiphiles but it seems that the ester linkages in the side groups which point

0040-6090/91/$3.50

towards the water act as the hydrophilic moiety while the helix is sufficiently hydrophobic to prevent these materials from being soluble in water.

Kawaguchi *et al.* reported the formation of X-type LB films of cellulose-esters with hydrophobic side groups[17,18]. These films appeared to be non-centrosymmetric and might be interesting for future applications in optoelectronic devices. However, LB films of cellulose-tridodecanoate could only be prepared using the horizontal lifting method. From structural studies of the multilayers of these cellulose tri-esters, it was concluded that the glucose units with β(1–4) linkages lie nearly flat on the water surface and the three vertical hydrocarbon chains attached to one glucose unit form a hexagonally packed ordered region. In the multilayer, the extended hydrocarbon chains are oriented perpendicular to the surface of the LB film.

The difference between amylose-esters and cellulose-esters is the linkage between the glucose units, an α(1–4) linkage in the case of an amylose-ester, a β(1–4) linkage in the case of a cellulose-ester. This difference in linkage has a great influence on the molecular conformation.

In this paper we present a study of the monolayer properties of amylose-esters with short alkyl side chains (amylose-acetate, amylose-propionate and amylose-butyrate), medium length alkyl side chains (amylose-laurate) and long alkyl side chains (amylose-palmitate). The transfer of these esters using the vertical dipping method was also studied. The structure of the LB multilayers was determined by grazing incidence reflection (GIR) and transmission IR spectroscopy, small-angle X-ray scattering (SAXS) and ellipsometry. A comparison will be made with the known structure of the crystalline films of amylose-esters as studied by Zugenmaier and Steinmeier[19].

2. EXPERIMENTAL DETAILS

The amylose-esters used in this study were synthesized following the method of Malm *et al.*[20] or the esterfication method with *N*-methylimidazole as a reaction medium[21]. A high molecular weight sample, amylose *V* from Avebe, was hydrolysed by dissolving the amylose in 10 wt.% sodium hydroxide at 90 °C. A 10 wt.% sulphuric acid solution was added until a pH of 1 was reached. This solution was stirred for 1 h at 90 °C and cooled down to room temperature. The residue was washed with distilled water until a pH of 7 was reached and the product was dried. The amylose was hydrolysed until a degree of polymerization of about 40 glucose units. Amylose-acetate, amylose-propionate, amylose-butyrate and amylose-palmitate 1 and 2 were synthesized by a one-step procedure in *N*-methylimidazole.

Hydrolysed amylose was dissolved in distilled *N*-methylimidazole at 90 °C with a concentration of 10 wt.%. The solution was cooled down to 5 °C and an excess of the corresponding anhydride or acid chloride was added dropwise to the amylose solution. The reaction mixture was stirred for 4 h at room temperature and the polymer was precipitated by pouring the mixture into methanol. The reaction product was purified two times by precipitation in methanol from chloroform solution (p.a. quality). The degree of substitution (DS) was determined by elemental analysis. In order to prepare amylose-palmitate with DS = 3, the above-described

procedure was followed twice. Amylose-laurate was synthesized according to the method of Malm *et al.*[20] (see Table I).

TABLE I
SYNTHESIZED POLYMERS

Polymer	*Code*	DS	*Molecular weight of the repeating unit*
Amylose-acetate	AAC	3.0	288
Amylose-propionate	APR	2.7	315
Amylose-butyrate	AB	2.7	353
Amylose-laurate	AL	2.6	643
Amylose-palmitate 1	AP1	1.7	574
Amylose-palmitate 2	AP2	2.3	721
Amylose-palmitate 3	AP3	3.0	877

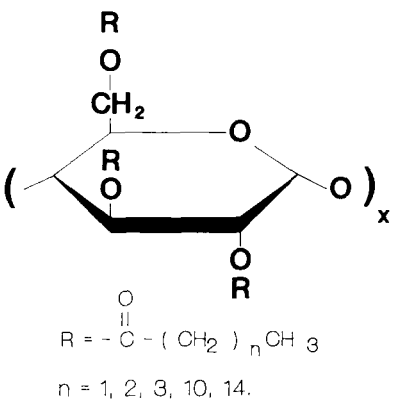

Monolayer properties were studied by pressure–area isotherms measured on a computer-controlled Lauda-Filmbalance (FW2). The subphase was purified water (doubly distilled followed by filtration through a Milli-Q purification system). The polymers were dissolved in chloroform (Uvasol quality) at concentrations of about 0.1 wt.%. Pressure–area diagrams were measured at different temperatures with a standard compression speed of 10 $Å^2$ molecular unit^{-1} min^{-1}. In order to elucidate the kinetic effects, isotherms were also measured at a lower speed (1 $Å^2$ molecular unit^{-1} min^{-1}). ZnS plates (Irtran, Spectra-tech), silicon wafers and gold layers on glass were used as substrates. The cleaning procedure of the silicon wafers was as follows: first the substrate was cleaned ultrasonically with chloroform and after drying it was treated with concentrated chromic acid for two hours at 80 °C, washed several times with Milli-Q water, washed ultrasonically with acetone and chloroform (all p.a. quality) dried and stored. Just before use, the substrate was rinsed with chloroform and partially hydrophobized by treatment of the substrates with a hexamethyldisilazane–chloroform solution at 50 °C. ZnS plates were ultrasonically cleaned with organic solvents. Gold substrates were prepared by

sputtering gold (thickness of ± 500 Å) onto glass slides with a Biorad Turbo-coater E6700.

Transfer experiments were carried out after stabilization of the monolayer on the water surface at constant temperature and pressure. All IR measurements were carried out using a Bruker IFS88 FTIR spectrophotometer with an MCT-A detector (D-313, Infrared Associates). The spectra were recorded with a resolution of 4 cm^{-1}. Grazing-incidence reflection spectra, with p-polarized light (perpendicular to the surface $E_{\perp}$[22,23]), were taken from multilayers on gold substrates. Transmission spectra with polarization parallel to the surface $E_{\parallel}$ were obtained from multilayers deposited onto both sides of a ZnS plate 2 mm thick. The multilayer spectra were taken using 4 cycles of 250 scans each according to the method of Arndt *et al.*[24] Transmission spectra with polarized radiation (0° and 90°) were obtained from the same multilayer. Spectra of isotropic samples of the polymers were obtained from films cast from chloroform solution onto KBr disks. It was checked if this method gave isotropic spectra by comparing the results with spectra measured from KBr pellets.

3. RESULTS AND DISCUSSION

3.1. Monolayer properties

Figure 1 shows pressure–area (π–A) isotherms of the amylose-esters with a high DS (DS $\geq$ 2.6) with various alkyl chains at 24 °C. Amylose-esters with short alkyl side chains all show the same kind of behaviour (curves A, B and C, Fig. 1), only the areas per molecular unit where the transitions take place differ. The laurate-ester and palmitate-ester show a completely different behaviour, which will be discussed further on.

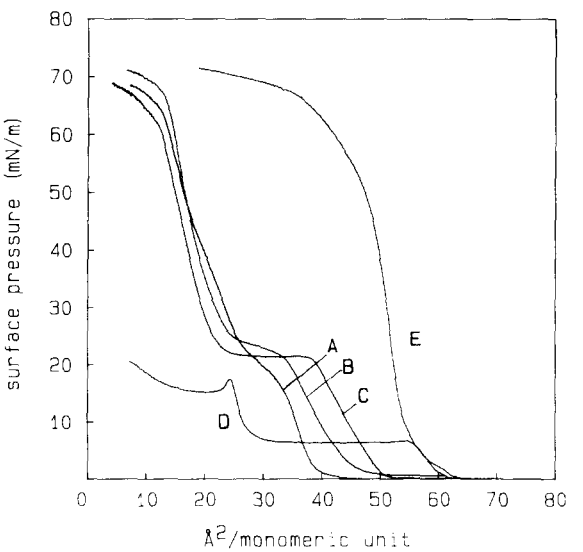

Fig. 1. Surface pressure–area isotherms of amylose-esters with high DS at 24 °C: A, amylose-acetate; B, amylose-propionate; C, amylose-butyrate; D, amylose-laurate; E, amylose-palmitate.

Figure 2 shows the temperature dependence of the isotherms of AAC. It appears that part of the isotherm ($\pi < 10\,\mathrm{mN\,m^{-1}}$) is independent of the temperature, whereas at higher surface pressure a considerable shift to lower area per monomeric unit occurs. The same effect was found for APR and AB. These isotherms were measured with a constant compression speed of $10\,\text{Å}^2$ monomeric unit^{-1} min^{-1} and additional kinetic effects might be present in these curves originating from slow processes in the monolayers. In Fig. 3 the effect of lower compression speed on the isotherm of AAC is shown for two temperatures. Apparently at higher temperatures the effect of the compression speed is of minor importance, but at lower temperatures a pronounced effect can be seen on that part of the isotherm, which also shows a pronounced temperature dependence (curves A and B). From these two sets of experiments it can be concluded that the isotherms of AAC (and also of APR and AB) can be divided in two parts: a part at low surface pressure where the isotherm is independent of temperature and compression speed and is without kinetic effect, and another part where considerable effects of both variables can be found, indicating that some kind of slow reorganization process may take place. More detailed information on both states can be found from stability experiments shown in Fig. 4. For AB (and APR and AAC) a momentary stable layer is found at surface pressures less than $10\,\mathrm{mN\,m^{-1}}$, whereas at higher pressures (second part of the isotherms) a slowly decreasing area is found. However, after a rather long period a stable state is also found, which would not be expected if some kind of collapse process were taking place.

AAC forms a stable monolayer when the units occupy an area of $38\,\text{Å}^2$. The occupied area per molecular unit is reduced to almost half the original layer ($22\,\text{Å}^2$) after the transition that takes place at $\pi = 23\,\mathrm{mN\,m^{-1}}$.

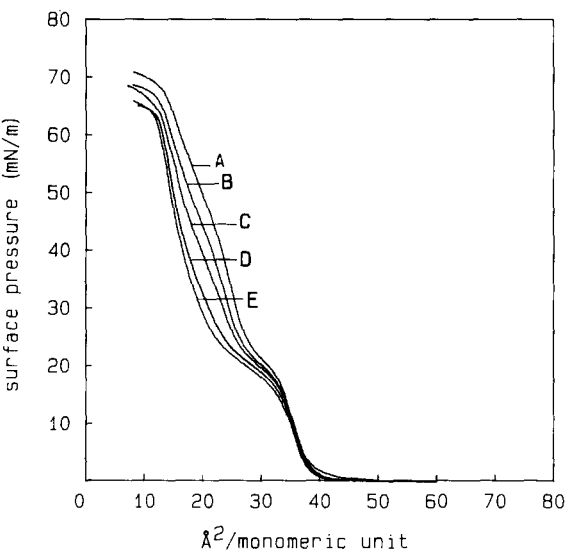

Fig. 2. Temperature dependence of the surface pressure–area isotherms of amylose-acetate: A, 10.3 °C; B, 15.5 °C; C, 23.5 °C; D, 32.9° C; E, 36.8 °C.

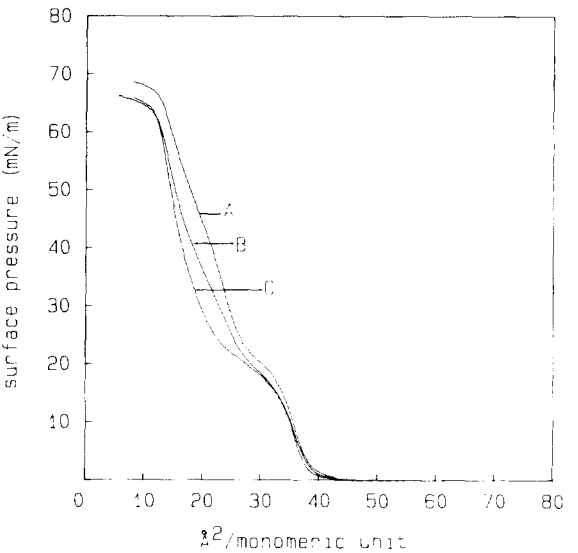

Fig. 3. Surface pressure–area isotherms of amylose-acetate with different compression speeds and temperatures. A, 15.5 °C, 10 Å^2 molecular unit^{-1} min^{-1}; B, 15.5 °C, 1 Å^2 molecular unit^{-1} min^{-1}; C, 36.8 °C, 10 and 1 Å^2 molecular unit^{-1} min^{-1}.

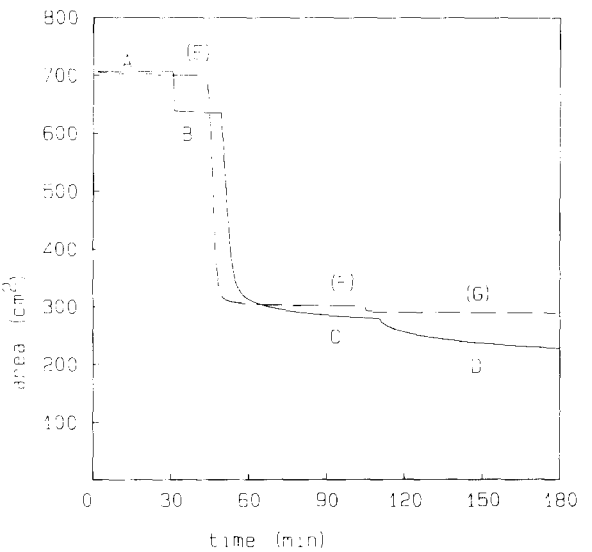

Fig. 4. Stabilization of a monolayer and a bilayer of amylose butyrate (——) and amylose-laurate (– – –) at the air–water surface at different surface pressures: A, 7 mN m^{-1}; B, 15 mN m^{-1}; C, 23 mN m^{-1}; D, 30 mN m^{-1}; E, 5 mN m^{-1}; F, 7 mN m^{-1}; G, 11 mN m^{-1}.

Considering the glucose unit as a three-substituted flat ring, the occupied area is in the range of 60 Å^2, as was found in the case of cellulose-esters reported by Kawaguchi *et al.*[17,18]. Zugenmaier and Steinmeier[19] determined the crystal structure of a homologous series of amylose-esters ranging from amylose-acetate to

amylose-valerate by X-ray studies combined with conformational energy calculations. According to a conformational study of crystalline amylose-acetate[19], the amylose-acetate chain was proposed to have a conformation of a 9/7 helix with a rise per residue of 3.78 Å and a diameter of approximately 10 Å, resulting in the value of 37.8 Å per glucose unit projected on a flat plane. This value agrees very well with the area found in the pressure–area curves in Fig. 1.

Amylose-propionate and amylose-butyrate also form stable monolayers. When the pressure is raised to a surface pressure of $\pi = 23\,\mathrm{mN\,m^{-1}}$, a transition also takes place (Fig. 1). One esterfied glucose unit of APR occupies $47\,\mathrm{Å^2}$ in a monolayer and 24 Å after the transition. The values for the amylose-butyrate polymer are slightly higher: $51\,\mathrm{Å^2}$ and $25\,\mathrm{Å^2}$ respectively. For the crystalline conformations it is calculated according to the data of Zugenmaier and Steinmeier that amylose-propionate occupies an area of $51\,\mathrm{Å^2}$ when it is projected on a flat plane, for an amylose-butyrate helix this value is $57\,\mathrm{Å^2}$, considering a 5/4 type helix with a rise per residue of 3.69 Å for both polymers.

We assume that the spread amylose-esters with short alkyl chains have the same helical conformation on the water surface as in the crystalline state. The discrepancy between the calculated values of the occupied areas for the glucose units and the value found in this study is probably due to experimental error. This is supported by the IR spectra and the SAXS data for the multilayers, discussed later on.

In the isotherms of AAC, APR and AB there is a plateau region at a well defined surface pressure, where the monolayers clearly undergo a transition. It is thought that this transition corresponds with the transition from a monolayer to a bilayer. Malcolm has also suggested these kinds of transitions for synthetic polypeptides[14]. The plateau region is considered to be a regular collapse of the helices on the water surface to a more or less stable bilayer. The reduction of the area per residue after the transition to half the initial value supports this idea.

According to the theory of bilayer formation given by Malcolm[14], a number of molecules in a monolayer under pressure are forced out of the layer and act as nuclei for the formation of the second layer. Once this has happened, the second layer will be formed as a cooperative process owing to attractive forces between the layers.

Figure 4 shows the formation of a monolayer and a bilayer of amylose-butyrate. The regions A and B in the figure correspond to the formation of a stable monolayer. As can be seen, these monolayers are almost instantaneously stable. When the pressure in the monolayer is raised to the transition pressure (Fig. 4, part C) the occupied area is reduced to half the initial area. At a pressure of $23\,\mathrm{mN\,m^{-1}}$ (Fig. 4, part C) the monolayer does not reach complete stability in the shown time. The minimum decrease in occupied area per time unit in Fig. 4 is determined to be $0.13\,\mathrm{mm^2\,min^{-1}}$. After at least 9 h the layer reaches an equilibrium state. This behaviour is representative for the amylose-esters with short alkyl chains. We could not transfer the more or less stable bilayer onto a solid substrate and because the bilayer could not be transferred to a solid substrate, the proposed structure is not confirmed by SAXS, or ellipsometric measurements.

Amylose-laurate is an example of an amylose-ester with a medium alkyl side chain. In order to investigate the monolayer properties of the laurate-ester the

temperature dependence of the π–A isotherms was measured. Figure 5 shows the result of these measurements. The side chains have a liquid-analogous conformation at low pressure ($\pi \leq 10\,\mathrm{mN\,m^{-1}}$), whereas above this pressure the side chains no longer stabilize the monolayer and a phase transition probaby takes place. The same kind of side chain behaviour is found for cellulose-laurate esters by Kawachuchi *et al*[17,18]. The laurate-ester changes to a stable state when the monolayer is compressed to an area of 25 $\mathrm{Å^2}$ per unit, as was verified by stabilization experiments like those in Fig. 4. We assume that this transition corresponds to the formation of a helical bilayer, as was found for the esters with short alkyl chains. In contrast to the amylose-esters with the short alkyl chains, the amylose-laurate polymer forms a completely stable layer at a pressure of $7\,\mathrm{mN\,m^{-1}}$ Fig. 4, part F) and $11\,\mathrm{mN\,m^{-1}}$ (Fig. 4, part G) in a short time. The stability is probably enhanced by the increase in attractive forces between the polymer chains of the amylose-laurate compared with the amylose-esters with the short alkyl chains at a low pressure. When the pressure is raised further, the more or less ordered layer collapses almost immediately because the medium alkyl chains do not have sufficient interaction with the water surface.

When the side chains are able to crystallize, as in the amylose-palmitate polymer, the monolayer behaviour is completely different, as can be seen in Fig. 6. At low temperatures ($T \leq 24\,^{\circ}\mathrm{C}$) there is no transition. When the molecules start to interact on a measurable scale, they form a condensed state with closely packed side chains. When the temperature is raised, the side chains are first in a liquid-analogous state and upon increasing the pressure a transition takes place to the condensed state.

One molecular unit occupying $\pm 60\,\mathrm{Å^2}$ corresponds with the area of a tri-substituted flat glucose ring and also to the cross-sectional area of three vertical

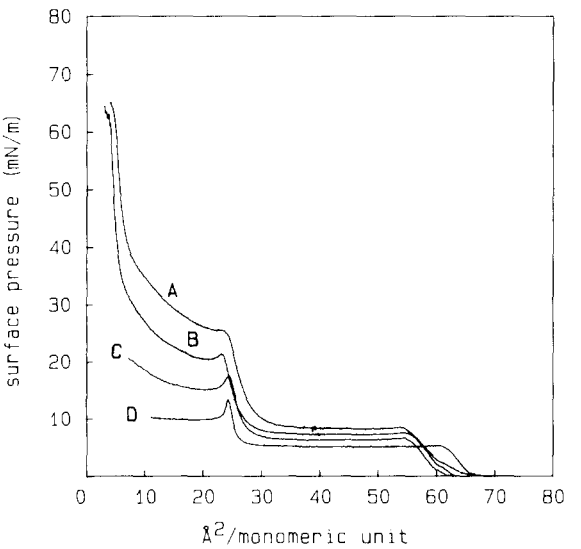

Fig. 5. The temperature dependence of surface pressure–area isotherms of amylose-laurate: A, 10.8 °C; B, 15.7 °C; C, 24.5 °C; D, 34.2 °C.

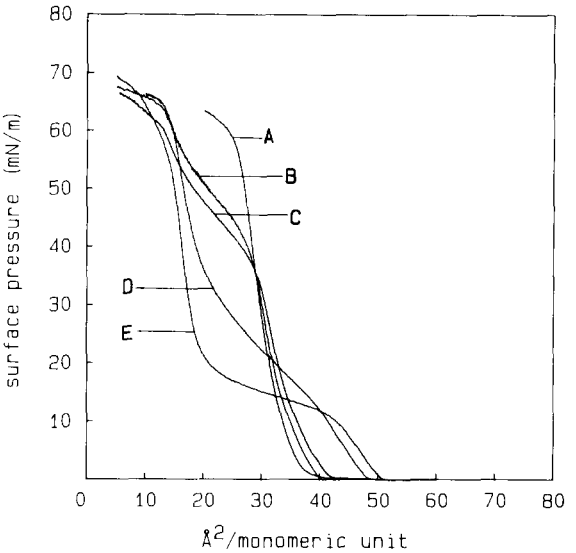

Fig. 6. Temperature dependence of surface pressure–area isotherms of amylose-palmitate (AP1): A, 10.8 °C; B, 24.1 °C; C, 25.8 °C; D, 31.7 °C; E, 36.8 °C.

hydrocarbon chains[17]. In order to elucidate the origin of the dimensions found for AP3, isotherms of amylose-palmitate esters with different degrees of substitution were measured. From the isotherms (not shown) of AP1, AP2 and AP3 with a DS of 1.7, 2.3 and 3.0 respectively, the cross-sectional areas were determined. In the condensed state the extrapolated cross-sectional areas are 34 Å^2, 44 Å^2 and 58 Å^2 respectively. It can be deduced from these data that the value of the area of one molecular unit is controlled by the side chains. The cross-sectional area per substituted alkyl chain is found to be almost constant for the amylose-palmitate esters (19 ± 1 Å^2).

We conclude from the π–A isotherms that the monolayer properties of the amylose-esters with short alkyl side-chains are mainly controlled by the backbone conformation. The behaviour of the isotherms of the medium and long chain amylose-esters is controlled by the side chains rather than the backbone.

3.2. Multilayers

Formation of multilayers on partially hydrophobic substrates using the vertical dipping LB technique could be achieved with the amylose-esters with short alkyl side chains and with amylose-palmitate with a DS of 1.7 (AP1). Transfer ratios were constant at least up to 50 layers under optimum conditions, as given in Table II.

It is thought that the extent of hydrophilicity is responsible for the type of transfer[25]. Amylose-acetate is the most hydrophilic monolayer, compared with the other amylose-esters used in this study, and is the only polymer that gives Z-type transfer. With increased hydrophobic properties of the monolayer, the transfer ratio on the down stroke increases, leading to more Y-type transfer. AP1 must exist to some extent in the liquid-analogous state to realize constant deposition, as was

TABLE II
TRANSFER PROPERTIES OF THE AMYLOSE-ESTERS

Polymer code	*Type of transfer*	*Transfer ratio*		*Temperature* (°C)	*Pressure* ($mN\,m^{-1}$)
		↓	↑		
AAC	Z	0.0	1.0	22–28	7
APR	Y	0.7	1.0	25	10–15
AB	Y	0.7	1.0	25	12–18
AP1	Y	0.9	1.0	25–30	15–20

found for other polymers[1,12,16]. For the higher substituted palmitate-esters, it was not possible to find suitable transfer conditions. The closely packed alkyl chains, together with the stiff polymeric backbone, apparently results in a rigid monolayer which prevents transfer. This phenomenon was studied in detail for various poly-octadecylmethacrylates[12].

3.3 Structural measurements

Bulk Fourier transform (FT)-IR spectra of an isotropic sample were compared with GIR spectra and transmission spectra of the multilayers. For GIR spectra it is known[22,23] that individual group vibrations, inducing dipole moment changes of this group, absorb strongly when these dipole moment changes are oriented perpendicular to the reflecting metal mirror.

Correspondingly, they will not absorb in the transmission spectra of the same structure, where the electric field vector of the light is parallel to the substrate.

Orientation of the molecules might also be deduced from transmission spectra obtained with polarized IR light, for instance perpendicular and parallel to the dipping direction. To our knowledge no detailed vibrational analysis of the amylose-esters has appeared in the literature. Band assignments have to be made by combining the results of other compounds.

Comparing the FT-IR spectra of amylose-acetate with the aforementioned different modes, differences can be seen if the bulk spectrum of AAC (film on KBr disc) is compared with the GIR-spectrum of AAC in the region 1200–800 cm^{-1}. Comparison of the GIR-spectrum of AAC with the bulk spectrum cannot be done directly because of dispersion effects which are present in the GIR-spectrum[27]. Figure 7(a) shows the calculated bulk spectrum of AAC in the GIR mode and the actually measured GIR spectrum.

The GIR bulk spectrum is calculated using the matrix formalism of Abèles[28]. The optical constants are calculated using the KBr spectrum of AAC of known thickness, a mean refractive index of 1.48 and the Kramer–Konig relationship[29]. The thickness of the KBr spectrum is calculated from the measured interference fringes of free-standing AAC films.

The orientation of AAC can be found in the absorption band at 1036 cm^{-1}, which is ascribed to a C—O—C vibration mode. However, this C—O—C bond is present in the glucose ring as well as outside the glucose ring as a connecting link between the glucose units. From a detailed investigation of the vibration spectra of

TABLE III
IR BAND ASSIGNMENTS

Vibration (cm^{-1})	→ *M*	*AAC1*	*APR1*	*AB1*	*AP1*
$\nu_a(CH_3)$	$\perp$ C—CH_3	2956	2962	2965	2957
$\nu_a(CH_2)$	$\perp$ C—C—C		2946	2937	2932
$\nu_s(CH_3)$	∥ C—CH_3		2878	2878	
$\nu_s(CH_3)$	∥ H—C—H				2852
$\nu_s(C{=}O)$	∥ C=O	1749	1745	1745	1744
$\delta_a(CH_2)$	∥ C—C—C		1463	1461	1465
$\delta_a(CH_3)$	∥ C—C—C	1432			
$\delta_s(CH_2)$			1421	1416	1413
$\delta_s(CH_3)$		1371	1380	1382	1377
Coupled motions of C—O—C vibrations from ester groups,		1237	1272 1175	1250 1171	1237 1164
Coupled motions of glucose units and linkages.		1165 1128 1036	1165 1087 1036	1090 1035	1115 1085 1030

ν, stretching bands; a, asymmetric; s, symmetric;
δ bending–deformation vibration.

pure amylose[30] it was concluded that the region below the 1500 cm^{-1} band is complex with coupled vibration modes, and therefore it is impossible to draw any definite conclusions about the precise orientations of the polymer chains in the LB layers. No orientation effects were found in the vibration absorbances above 1200 cm^{-1}.

Figure 7(b) shows the transmission spectra of AAC on Irtran-2 substrates with two different polarizations of the IR beam. Distinct differences can be seen between two spectra in the 1300–800 cm^{-1} region. The other part of the spectra did not show any changes. From this we may conclude that in these LB-multilayers, orientation of the polymer molecules occurs, whereas the orientation of the ester side chains is not found because in all cases the absorption of the C=O group at 1749 cm^{-1} remained constant.

From these polarized transmission spectra it follows that there is an orientation of the polymer backbone towards the dipping direction.

The dichroic measurements agree with the idea of the helical conformation of the amylose-acetate in the LB layers. In a helical conformation, a dichroic effect can only be expected when the absorbing vibration is fixed in the conformation. Freely rotating groups are expected to have a random distribution. Comparing the GIR spectrum with the transmission spectrum using light polarized perpendicular to the dipping direction, the absorption at 1036 cm^{-1} changes in the same way. This can be explained by the suggested model of oriented helices. Both spectra detect the helices from the same point of view, *i.e.* perpendicular to the helix axis. Moreover, the same IR dichroic results were obtained by uniaxial stretching of a bulk amylose-acetate film.

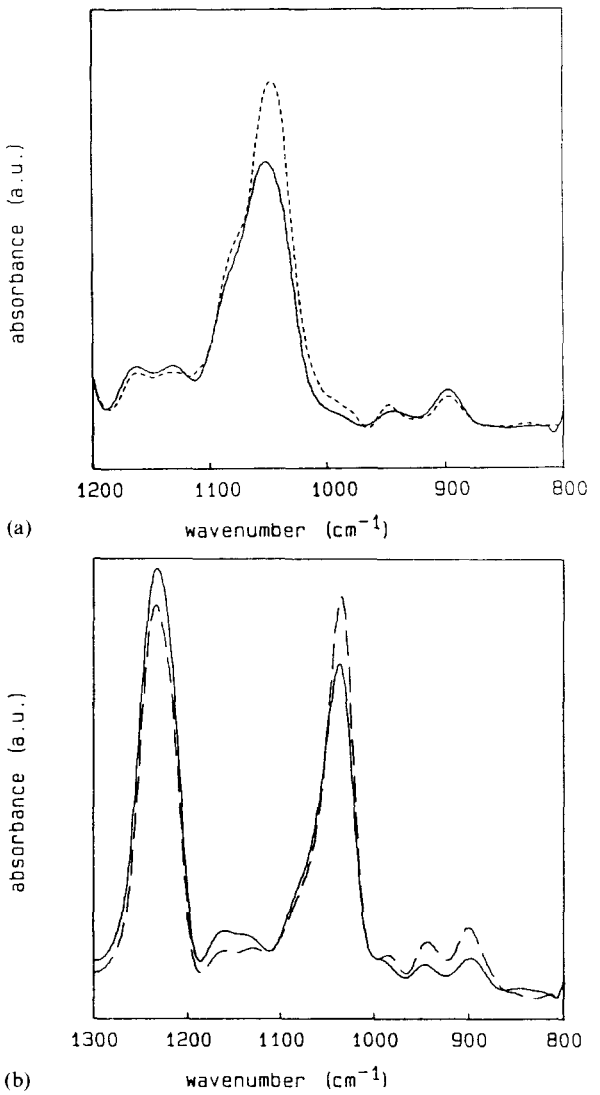

Fig. 7. (a) IR spectra of amylose-acetate: ——, GIR spectrum of 15 LB multilayers on a gold substrate; – – –, calculated GIR spectrum of a bulk sample of amylose-acetate. (b) Transmission spectra of LB layers consisting of 15 monolayers of amylose-acetate on each side of a ZnS plate: ——, polarized light perpendicular to the dipping direction; – – –, polarized light parallel to the dipping direction.

The amylose-propionate polymer and the amylose-butyrate polymer show the same tendency in the dichroic spectra as the amylose-acetate polymer. Polarized transmission IR measurements of the propionate and butyrate polymer did not show any preferential orientation, which is probably due to the incomplete down-stroke transfer (Table II).

In Fig. 8(a) the grazing angle spectra of 15 LB multilayers of amylose-palmitate (AP1) before (solid line) and after heating (dotted line) are shown. For comparison,

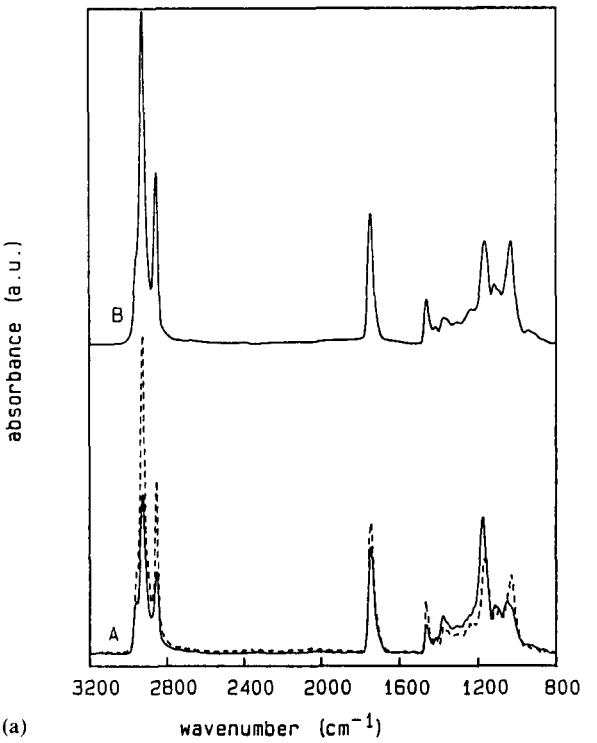

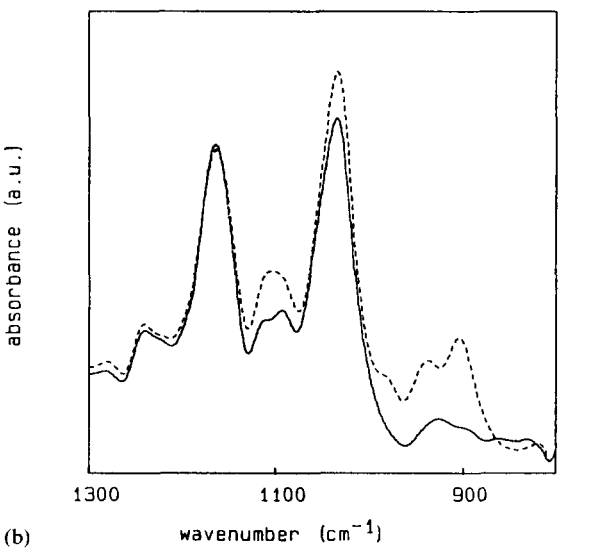

Fig. 8. (a) IR-spectra of amylose-palmitate (A): ——, GIR spectrum of 15 layers of amylose-palmitate on a gold substrate as deposited; – – –, GIR spectrum of the same multilayer after heating for 16 h at 120 °C; (B), KBr bulk spectrum. (b) Transmission IR spectra of amylose-palmitate: ——, 15 LB multilayers on each side of a ZnS plate, with polarized light perpendicular to the dipping direction; – – –, 15 LB multilayers on both sides of a ZnS plate with polarized light parallel to the dipping direction.

the KBr bulk spectrum is given (8a (B)). The dispersion of the refractive index had no measurable effect on the reflection spectrum as was calculated.

Of particular interest in these spectra is the CH_2 stretching region (3000–2800 cm^{-1}). The stretching vibrations ν_a (CH_3) at 2957 cm^{-1}, ν_a (CH_2) at 2932 cm^{-1} and ν_s (CH_2) at 2852 cm^{-1} show a decrease of about 47% in the GIR spectrum compared with the bulk spectrum. After heating the sample for 16 h at 120 °C the GIR spectrum changes to that given by the dashed line in Fig. 8(a). This spectrum coincides with the bulk spectrum B, indicating that the original orientation of the molecules has completely disappeared. From these measurements it follows that the CH_2 chains of the amylose-palmitate polymer have a preferential orientation perpendicular to the substrate, which disappears upon heating. Contrary to the amylose-esters with short alkyl chains, where only the absorption bands of the C—O—C vibrations deviate in the dichroic spectra, almost all bands in the amylose-palmitate polymer deviate from the bulk spectrum. This indicates that the glucose ring also has a specific orientation.

Transmission spectra with different polarizations of the IR beam are shown in Fig. 8(b). The most striking difference between the polarizations perpendicular (solid line) and parallel (dotted line) to the dipping direction are the ring breathing vibrations at 945 cm^{-1} and 905 cm^{-1}. Also the C—O—C bands show some dichroic effect. From these spectra it follows that there might be a small orientation of the backbone of the molecule in the dipping direction.

Multilayers of amylose-esters with short alkyl chains do not show any reflection in the SAXS experiments. Because of this absence of reflections in the SAXS experiments, ellipsometric measurements were carried out to determine the thickness of the layers of the amylose-esters. The results are given in Table IV. The thicknesses appear to agree reasonably well with the estimated diameter of the corresponding crystalline helices when the incomplete transfer of APR and AB is also taken into account. The calculated thickness of one layer varies a little with the total thickness of the layer, as can be seen in Table IV. This can not be explained by irregular transfer. At this moment we can not give a suitable explanation.

TABLE IV

THICKNESS OF THE MULTILAYERS OF THE AMYLOSE-ESTERS WITH SHORT ALKYL SIDE CHAINS

Polymer	*Number of deposited layers*	*Transfer* ↓	↑	*Total thickness* (Å)	*Thickness of one layer* (Å)	*Crystal line thickness*[a]
AAC	15	0	1.0	136 ± 4	9.1	10.1
	20	0	1.0	184 ± 2	9.2	
APR	20	0.7	1.0	202 ± 2	11.8	10.8
	36	0.7	1.0	304 ± 8	9.9	
AB	20	0.7	1.0	208 ± 4	12.2	11.8
	40	0.7	1.0	387 ± 10	11.4	
API	40	0.9	1.0	836 ± 9	22.0	—

[a]Average thickness of one helix in the crystalline unit cell, as computed by Zugenmaier and Steinmeier[19].

SAXS experiments of amylose-palmitate mulitalyers do not show any reflections either. From ellipsometric measurements the thickness of one layer was determined to be 22 Å. This value almost corresponds to a stretched CH_2 chain of 15 carbon atoms. A fully stretched chain has a length of 19 Å. This result corresponds with the IR data, although the layer is not regular enough to give X-ray reflections. The lack of X-ray reflections may arise from the fact that the multilayers are prepared by transferring monolayers in the liquid-analogous state.

Finally, the results are combined in Fig. 9, showing a schematic representation of the proposed structure of the LB fims of the amylose-esters with the short alkyl chains and the long alkyl chains.

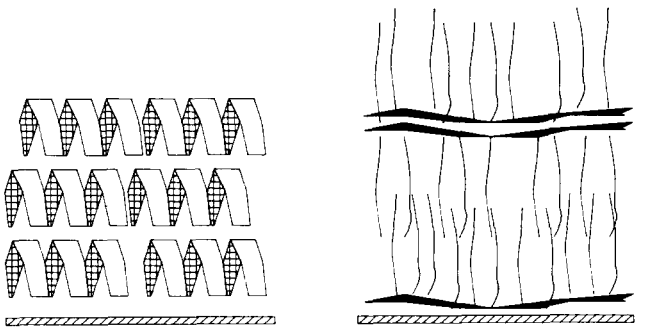

(a) (b)

Fig. 9. Schematic representation of the proposed structure of the LB-films: (a) LB film of amylose-esters with short alkyl chains; (b) LB film of amylose-esters with long alkyl chains.

4. CONCLUSIONS

Monolayer properties of a series of amylose-alkylesters were studied and it was found that amylose-esters with short alkyl side chains form helices on the water surface. The dimensions of the helices on the water surface agree with the corresponding crystalline polymers reported by Zugenmaier and Steinmeier[19]. A transition from a stable monolayer to a bilayer was observed. The monolayer properties of the amylose-esters with medium and long alkyl side chains were controlled by the side chains rather than by the backbone. The side chains of the amylose-laurate polymer were not able to crystallize. In contrast to the laurate-ester, the palmitate side chains do crystallize on the water surface causing a condensed state. Multilayers of amylose-acetate, amylose-propionate, amylose-butyrate and the palmitate with a DS of 1.7 could be prepared up to at least 50 monolayers. The amylose-acetate polymer formed Z-type layers with a transfer ratio of unity and the helical conformation is conserved in the multilayer. Moreover, a preferential orientation of the helices parallel to the dipping direction could be deduced from the dichroic IR spectra. The other polymers showed more or less Y-type transfer.

Polarized IR measurements and X-ray diffraction of the amylose-palmitate polymer revealed a more or less ordered structure with a preferential orientation of the alkyl chains perpendicular to the surface.

ACKNOWLEDGMENTS

We greatly acknowledge the financial support by AKZO NV, The Netherlands, for this research project.

We like to thank Richard Brinkhuis for making the FT-IR simulation computer program and for helpful discussions.

REFERENCES

1 G. Duda, A. J. Schouten, T. Arndt, G. Lieser, G. F. Schmidt, C. Bubeck and G. Wegner, *Thin Solid Films*, *159* (1988) 221.
2 M. B. Biddle, J. B. Lando, H. Ringsdorf, G. Schmidt and J. Schneider, *Colloid Polym. Sci*, *266* (1988) 806.
3 M. Watanabe, Y. Kosaka, K. Oguchi, K. Sanui and N. Ogata, *Macromolecules*, *21* (1988) 2997.
4 J. R. Katz and P. J. P. Samwell, *Ann. Chem.*, *472* (1924) 241.
5 D. J. Crisp, *J. Colloid. Sci.*, *1* (1946) 1, 161.
6 R. H. Tredgold and C. S. Winter, *J. Phys. D*, *15* (1982) L55.
7 R. H. Tredgold and C. S. Winter, *Thin Solid Films*, *99* (1983) 81.
8 S. J. Mumby, J. D. Swalen and J. F. Rabolt, *Macromolecules*, *19* (1986) 1054.
9 R. Elbert, A. Laschewsky and H. Ringsdorf, *J. Am. Chem. Soc.*, *107* (1985) 4134.
10 J. Schneider, H. Ringsdorf and J. F. Rabolt. *Macromolecules*, *22* (1989) 205.
11 J. Schneider, C. Erdelen, H. Ringsdorf and J. F. Rabolt. *Macromolecules*, *22* (1989) 3475.
12 A. J. Schouten, G. Wegner, submitted for publication in *Thin Solid Films*.
13 R. H. Tredgold, *Thin Solid Films*, *152* (1987) 223.
14 B. J. Malcolm, *Proc. R. Soc. London, Ser. A*, *305* (1968) 363.
15 C. S. Winter and R. H. Tredgold, *Thin Solid Films*, *123* (1985) L1.
16 G. Duda, *Ph.D. Thesis*, Mainz, 1988.
17 T. Kawaguchi, H. Nakahara and K. Fukuda, *Thin Solid Films*, *133* (1985) 29.
18 T. Kawaguchi, H. Nakahara and K. Fukuda, *J. Colloid. Interface Sci.*, *104* (1985) 209.
19 P. Zugenmaier and H. Steinmeier, *Polymer*, *27* (1986) 1601.
20 C. J. Malm, J. W. Mench. D. L. Kendal and G. D. Hiatt, *Ind. Eng. Chem.*, *43* (1951) 684.
21 R. Wachwiak and K. A. Conners, *Anal. Chem.*, *51* (1979) 27.
22 R. G. Greenler, *J. Chem. Phys.*, *44* (1966) 310.
23 T. Arndt, *Ph.D. Thesis*, Mainz, 1988.
24 T. Arndt, C. Bubeck, A. J. Schouten G. Wegner. *Mikrochim. Acta*, *II* (1988) 7.
25 R. Popovitz-Biro, K. Hill, E. M. Lahav, L. Leiserowitz, J. Sagiv, H. Hsiing, G. R. Meredith and H. Vanherzeele, *J. Am. Chem. Soc*, *110* (1988) 2672.
26 T. Arndt, A. J. Schouten, G. F. Schmidt and G. Wegner, submitted for publication to Makromol. Chem.
27 R. T. Graf, J. J. L. Koenig and H. H. Ishida, *Pol. Prepr.*, *25* (1984) 188.
28 F. Abèles, *Ann. Phys.*, *12* (1948) 33.
29 D. L. Allara, A. Baca and C. A. Pryde., *Macromolecules*, *11* (1978) 1215.
30 M. Mthlouthi and J. L. Koenig, *Advances in Carbon Chemistry and Biochemistry*, Academic Press, Orlando FL, 1986, Vol. 44, p. 7.